Modeling and simulation for energy coupling for laser-material interaction
Jiang, Hongjun; Woodard, Paul

National Research Council Canada   Conseil national de recherches Canada

Canada

IMTI ITFI Publication

Integrated Manufacturing Technologies Institute

Institut des technologies de fabrication intégrée

Modeling and Simulation of Energy Coupling for Laser-Material Interaction

Hongjun Jiang
Paul Woodard

National Research Council of Canada   Conseil national de recherches du Canada

Pages: ___20___

**REPORT
RAPPORT**

Date: _March 2003_____

Fig.
Diag. _____

SAP Project #
de Projet de SAP_____

For
Pour _____

_____Unclassified_____
(Classification)

IMTI-TR-012 (2003/02)

**Modeling and Simulation of Energy Coupling
for
Laser-Material Interaction**

Submitted by
Présenté par _____Paul Woodard_____
                        Group Leader

First Author
Auteur Premier_____Hongjun Jiang_____

Approved
Approuvé _Gian Vascotto_____
                   Director

b20084407 BB

IMTI PUBLICATION AND PRESENTATION APPROVAL FORM

This form **must** be completed and given to Administration **before** a manuscript or presentation abstract is submitted.

1. General information (Please Print)

Author(s) (listed in the order in which they will appear in the citation):

Author	Signature	Date
Hongjun Jiang	H. Jiang	Jan. 14/03
Paul Woodard	Paul Woodard	13-Feb/03

Title: Modeling and Simulation of Energy Coupling for Laser-Material Interaction

Publication to which paper will be submitted (indicate charges if applicable):

_____

_____

Name, date and location of conference presentation:

_____

_____

2. Approval

	Signature	Date
Submitted by:	Paul Woodard	13/Feb/03
Reviewed by:	Paul Woodard	13/Feb/03
Edited by:	Roberto Camas	13/Feb/03
Approved by Director:		Feb. 18/03

3. Category (this section to be completed by Director)

Please check one of the following:

- [ ] Journal Paper (Refereed)
- [ ] Journal Paper (Non-refereed)
- [ ] Conference Proceedings (Ref.)
- [ ] Conference Proceedings (Non-ref.)
- [x] TR
- [ ] GR

- [ ] Book/Book Chapter
- [ ] Presentation
- [ ] Institute/Technical/Client Report
- [ ] Article in Trade Magazine
- [ ] CTR
- [ ] Other (specify)

unclass
unlim.

IMTI-TR-012 (2003/02)

Modeling and Simulation of Energy Coupling for Laser-Material Interaction

Hongjun Jiang and Paul Woodard
Integrated Manufacturing Technologies Institute, National Research Council of Canada
800 Collip Circle, London, ON, N6G 4X8, Canada

Abstract
Energy coupling is a key phenomenon in material processing techniques that use lasers. It is a complex physical process, which involves numerous parameters, such as material's refractive index, laser wavelength, angle of incidence, polarization, temperature, power, power intensity, surface roughness and surface coating. Although there are some empirical and theoretical models of the dependence of the energy coupling efficiency (also known as absorptivity) on individual and/or groups of parameters, to date, there is no comprehensive model that addresses the wide array of parameters that affect energy coupling for laser material interaction.

To address this need, several of the available models are examined, and a generic methodology is introduced and used to de-couple, classify and regroup the parameters. A model that combines the influences of the selected parameters is described. Several simulations are conducted to demonstrate the utility of the generic model, and the current limitations of the new model are addressed.

Both spatial and temporal distributions of the absorptivity are simulated and effects of selected parameters on distribution and magnitude of the absorptivity have been investigated by using the model. Simulation results and comparisons to published results are made, and some new findings are presented.

Keywords: laser material interaction, energy coupling efficiency, absorptivity, generic model, simulation

Nomenclature

A		Absorptivity of material surface
A_p		Absorptivity of material surface under P- polarized laser radiation
A_s		Absorptivity of material surface under S- polarized laser radiation
R		Reflectivity of material surface
R_p		Reflectivity of material surface under P- polarized laser radiation
R_s		Reflectivity of material surface under S- polarized laser radiation
$\tilde{n}$		Complex refractive index, $\tilde{n} = n + ik$
$\tilde{\varepsilon}$		Complex dielectric constant, $\tilde{\varepsilon} = \varepsilon_1 + i\varepsilon_2$
φ	°	Angle of incidence

TEM_{plq}		Transverse Electromagnetic Mode. p = number of radial zero fields; l=number of angular zero fields; q=number of longitudinal zero fields
d_{min}	mm	Diameter of focal spot size
$\sigma(z)$	mm	Standard deviation of power intensity distribution
D_{adz}	mm	Diameter of absorptivity distributed zone
P	W	Power for continuous wave laser light
$\overline{P}$	W	Average value of power for pulse wave laser light
I	W/mm^2	Laser power intensity
I_0	W/mm^2	Laser power intensity at point (0,0)
t	s	Time
τ_1	s	Rise-up duration for saw-toothed pulse wave
τ_2	s	Fall-down duration for saw-toothed pulse wave
τ	s	Pulse period for saw-toothed wave
f	mm	Focal length
D	mm	Unfocused beam diameter
λ	mm	Laser wavelength
T	°C	Surface temperature
x,y,z	mm	Cartesian coordinates
SP(x,y)		Spatial distribution function

1. Introduction

Understanding of the laser-material interaction is fundamental for any laser machining process, such as cutting, welding, drilling, grooving, marking or scribing. The amount of energy transferred from laser light to a material's surface is determined by numerous parameters, such as the material itself and the associated properties of the material (surface roughness, material refractive index, etc), laser light wavelength, angle of incidence, polarization, temperature, and laser power intensity. This interaction between photon energy from a laser and a material are among the most fundamental of physical processes, and while models have been developed to simulate portions of this interaction, the process of laser parameter development still largely relies on informed trial and error.

The effect of changes in these parameters on the energy coupling efficiency (usually called absorptivity and defined as the ratio of the energy absorbed by the material to the incident laser energy) has long been the subject of investigation. Sub-models have been created for individual parameters or blocks of parameters, which will be reviewed in the following session. Despite this effort, a complete model that considers the influence of the bulk of the parameters as a whole is not available. It is believed that such a complete model would allow for better laser parameter and material selection for a wide range of laser processing applications.

In this paper, some of these individual models for laser material interaction are reviewed. The relationship between parameters is analyzed and two new intermediate models to simulate

absorptivity are created using a generic methodology. This generic methodology is part of a research effort to build sophisticated simulation tools from more fundamental models and equations. Using this approach, a model is built by combining the intermediate models to couple the numerous distinct models.

The paper describes the development of this model, and provides some simulation results. Anticipated limitations of this generic model are discussed and validations of the model as well as the simulation results are also presented.

2. Modeling of laser material interaction effects

As previously mentioned, numerous physical factors affect the absorptivity of laser energy by a material. Surface coating and surface roughness have effects on energy coupling of laser material interaction [1-3], but a systematical representation and modeling of these effects has been impeded by weak reproductivity of the same coating or same surface roughness. Other factors, such as material's refractive index, laser wavelength, angle of incidence and polarization, temperature, power intensity, TEM mode, and focal spot size, have been sufficiently studied. Their influences will be included in a generic model in this paper.

The absorptivity of a material on a flat surface under normal incidence of laser can be defined as the function of material's refractive index, and can be represented as [1,4]:

$$A = \frac{4n}{(n+1)^2 + k^2} \tag{1}$$

For an opaque material, such as most metals under typical light wavelengths, the reflectivity R is equal to 1-A. Values of n and k depend on laser wavelength and the temperature of the material's surface. The values of n, k and R of some commonly used metals can be found in Steen's book [1]. However in reality, little data is available at high temperature. Fortunately, a solution was provided by relating n and k to other material properties such as electrical conductivity and dielectric constant, which was presented in Duley's review [4].

Laser wavelength has an influence on absorptivity for many materials. The materials include not only metals, such as copper, iron, or nickel, but also metal oxides, such as ZrO_2 and Al_2O_3 or even organic material, such as FR4 [1,2,5,6]. Experimental results show that for all of the above materials, the absorptivity increases when laser frequency varies from infrared wavelength to ultraviolet wavelength. The reason was that at ultraviolet wavelength, more energetic photons could be absorbed by a greater number of bound electrons than that at infrared wavelength [1].

Theoretical analysis of the absorptivity allowing for angle of incidence shows a variation both with angle and the plane of polarization. The absorptivity for P- and S- polarized radiations absorbed by perfectly flat surfaces is given by:

$$\begin{cases} A_{P\text{-}nk\varphi} = \dfrac{4\dfrac{n}{\cos\varphi}}{\left(n + \dfrac{1}{\cos\varphi}\right)^2 + k^2} \\[6mm] A_{S\text{-}nk\varphi} = \dfrac{4n\cos\varphi}{(n + \cos\varphi)^2 + k^2} \end{cases} \qquad (2)$$

As an example, variation of reflectivity R_S (=1-A_S) and R_p (=1-A_P) of steel versus angle of incidence under the laser radiation of 1.06μm wavelength can be found in Fig.2.9 of Steen's book [1]. It shows that as φ increases from 0°, R_S increases smoothly and until it becomes unity at 90°. Similarly, R_P initially drops to a finite value, then increases until it becomes unity when φ is equal to 90°. A metal and a dielectric material at the wavelength of 10.6μm were found to have the similar variation of R_P and R_S with angle of incidence, as seen in Fig4.4 and Fig.4.5 in Migliore's book [7]. This phenomenon was believed to be similar for most opaque materials at most wavelengths.

As the temperature of a material's surface rises there will be an increase in the photon population, causing more photon-electron energy exchanges. Thus the electrons are more likely to interact with the material structure rather than oscillate and reradiate. There is thus a fall in the reflectivity and an increase in the absorptivity with a rise in temperature as seen in Fig.2.6 of Ref. [1]. Usually, this was followed by a plateau and possibly a successive decline of the absorptivity. A similar phenomenon has been found for P- and S- polarized laser lights, which is seen as Fig.4.10 in Duley's book [3]. Several models were available for the effect of temperature. Duley suggested that for many metals under infrared wavelength, absorptivity versus temperature could be approximated well by a linear function [4]. Dekumbis et al. obtained similar findings within the low temperature range in the study [8]. Furthermore, the variation of absorptivity with time (transient status) was also studied under different temperatures at oxidizing atmosphere [9].

Power intensity of laser has a great influence on absorptivity of material's surface. When the focused power density is not high enough, absorption will be low due to the high reflectivity of the surface. As power intensity increases, the rate or absorption of individual photons will increase, and thus, absorptivity will increase remarkably. Beyond a threshold of power intensity, absorptivity keeps at a constant value or decreases slightly. An exponential function was suggested to represent this relation for metals in Fuerschbach' study [10].

TEM is an acronym of Transverse Electromagnetic Mode of laser, which describes the distribution of energy in a laser beam [1]. TEM_{00}, also named as a Gaussian beam, is the simplest one and is commonly used to model the process of cutting, welding or drilling. Lasers with high rank mode beams are useful for surface marking and for fabricating micro apparatus. TEM mode determines the distribution of laser power intensity, which is as seen in Fig.2.13 of Ref. [1]. Therefore, it has a circuitous effect on the absorptivity, which will be modeled using functional analysis in this paper.
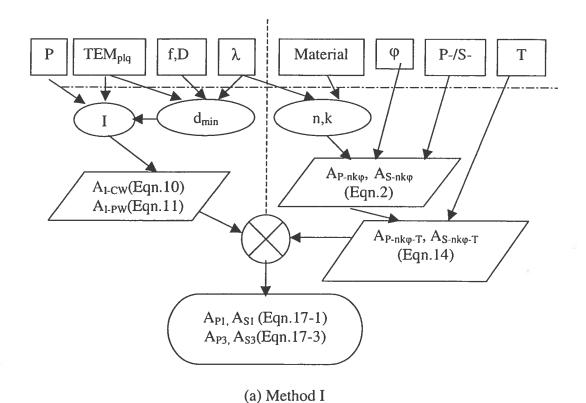
Focal spot size, d_{min} is an important parameter because it determines the mean volume of power intensity. Similar to TEM, d_{min} has a circuitous influence on the absorptivity of metal surface because of its influence on the power intensity. Also, this influence will be modeled using functional analysis in this paper.
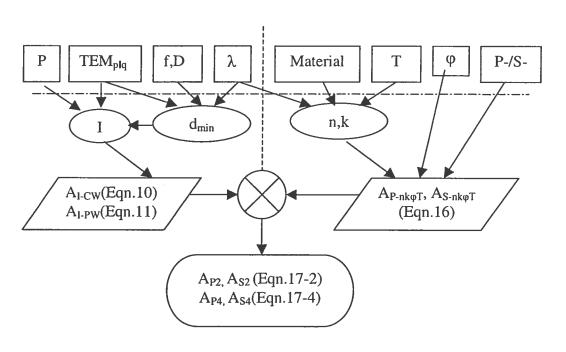
3. Generic model of laser material interaction

There are many parameters, including material's refractive index, laser wavelength, angle of incidence, polarization, temperature, power, power intensity, TEM mode, focal length, unfocused beam diameter, focal spot size, surface roughness and surface coating which have influences on energy coupling for laser-material interaction. A few sub-models including individual or some parameters, which may or may not be independent are available. The intention of the paper is to develop a generic model, which includes the first 11 parameters mentioned above. It is expected to inspect the comprehensive effects of all the parameters in a single model.

The methodology of generic modeling adopted here is to first analyze the relation of the parameters. These parameters were decoupled. Individual parameters were classified into two groups: primary parameters, which are listed above the dot-and-dash line as seen in Fig.1 and derivative parameters, which appear in the circles, underneath the dot-and-dash line. These parameters were then re-organized in two groups: power intensity related parameters and power intensity non-related parameters, which were shown in different side of the dash line in Fig.1. Effects of these two groups on absorptivity were independent. Two intermediate models were built independently.

Because two intermediate models have independent effects on absorptivity of laser-material energy coupling, the comprehensive effect included in the generic model was, therefore, equal to the algebraic product of two intermediate models. This method works in this case because one of the intermediate models acts as a shape function, with near constant magnitude. If the magnitude of the intermediate model was not near unity, a more complex convolution of the two models would be required.

P | TEM$_{plq}$ | f,D | λ | Material | φ | P-/S- | T

I | d$_{min}$ | n,k

A$_{I-CW}$(Eqn.10)
A$_{I-PW}$(Eqn.11)

A$_{P-nk\varphi}$, A$_{S-nk\varphi}$
(Eqn.2)

A$_{P-nk\varphi-T}$, A$_{S-nk\varphi-T}$
(Eqn.14)

⊗

A$_{PI}$, A$_{SI}$ (Eqn.17-1)
A$_{P3}$, A$_{S3}$(Eqn.17-3)

(a) Method I

P | TEM$_{plq}$ | f,D | λ | Material | T | φ | P-/S-

I | d$_{min}$ | n,k

A$_{I-CW}$(Eqn.10)
A$_{I-PW}$(Eqn.11)

A$_{P-nk\varphi T}$, A$_{S-nk\varphi T}$
(Eqn.16)

⊗

A$_{P2}$, A$_{S2}$ (Eqn.17-2)
A$_{P4}$, A$_{S4}$(Eqn.17-4)

(b) Method II
Fig.1 Process of generic modeling

3.1). Intermediate model I—effects of I, TEM_{plq} and d_{min}

3.1.1). Description of laser power intensity

For continuous wave (CW) laser radiation and with laser power intensity constant with time, the power intensity, I on material surface can be described as:

$$\begin{cases} I(x,y)=I_0 SP(x,y) \\ P=\iint_{x\ y} I(x,y)dxdy \end{cases} \tag{3}$$

Where, I_0 is the magnitude of the intensity at point (0,0), and $SP(x,y)$ is the spatial distribution of laser energy and is a function of x and y. $SP(x,y)$ can be any complex spatial distribution, integrated with mode patter information. However, it usually takes form of Gaussian distribution with a circular pattern, since TEM_{00} beams are most commonly used to model the laser processing applications. In this condition, power intensity can be represented as [11]:

$$I(x,y)=\frac{P}{2\pi\sigma^2(z)}\exp\left(-\frac{x^2+y^2}{2\sigma^2(z)}\right) \tag{4}$$

Where, $\sigma(z)$ is the standard deviation of the distribution, proportional to the beam diameter. If material surface locates on the focal plane (z=0), it is equal to half of the focused beam diameter, d_{min}, which is given by:

$$\begin{cases} \sigma(0)=\frac{d_{min}}{2} \\ d_{min}=2.44\frac{f\lambda}{D}(2p+1+1) \end{cases} \tag{5}$$

Otherwise,

$$\sigma(z)=\sigma(0)\sqrt{1+\left(\frac{\lambda z}{\pi\sigma^2(0)}\right)^2} \tag{6}$$

Where, z is the distance from material surface to the focal plane.

In the case where the laser beam was focused on the material surface, the power intensity distribution of a TEM_{00} beam can be represented as:

$$I(x,y)=\frac{PD^2}{2.98\pi f^2\lambda^2}\exp\left(-\frac{D^2}{2.98f^2\lambda^2}(x^2+y^2)\right) \tag{7}$$

If the laser operates in a pulsed wave (PW) mode, laser intensity varies with time. I_0 and $I(x,y)$ in Eqn.3 should be replaced by $I_0(t)$ and $I(x,y,t)$. $I_0(t)$ can vary as any function, determined by

the laser system. In this paper, it was assumed to be a saw-toothed wave function shown in Fig.2. Given the rise-up duration τ_1, fall-down duration τ_2, pulse period τ and laser power P (mean value), I(x,y,t) can be expressed as:

$$I(x,y,t)=\begin{cases}\dfrac{PD^2}{1.49\pi f^2\lambda^2}\dfrac{\tau(t-m\tau)}{\tau_1(\tau_1+\tau_2)}\exp\left(-\dfrac{D^2}{1.49f^2\lambda^2}\left(x^2+y^2\right)\right),m\tau<t\le m\tau+\tau_1\\[4mm]\dfrac{PD^2}{1.49\pi f^2\lambda^2}\dfrac{\tau(m\tau+\tau_1+\tau_2-t)}{\tau_2(\tau_1+\tau_2)}\exp\left(-\dfrac{D^2}{1.49f^2\lambda^2}\left(x^2+y^2\right)\right),m\tau+\tau_1<t\le m\tau+\tau_1+\tau_2\\[4mm]0,m\tau+\tau_1+\tau_2<t\le(m+1)\tau\end{cases}\quad(8)$$
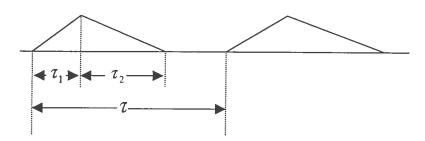
Where, m is an integer.

Fig.2 A saw-toothed laser pulse wave

3.1.2). Effects of power intensity on absorptivity

Fureschbach studied the Energy Transfer Efficiency (as the same meaning as absorptivity in this paper) for three metals, 1018 steel, tin and 304 stainless steel. Experimental results revealed that the absorptivity of three metals was exponentially related to the power intensity and this relationship can be expressed as:

$$A(I)=a-be^{-\frac{1}{k}}\qquad\qquad(9)$$

Where, a, b and k are constants, which were obtained by curve fitting. In Fureschbach's study, laser intensity was referred to the ratio of laser output power to the focused spot diameter, and the constants a, b and k were equal to 0.86, 1.4 and 11.0kW/cm respectively [10]. No obvious difference of the value of a, b and k was observed for three materials in Fureschbach's study. Whether it varies with other materials, however, has to be identified by further investigations.

Usually, the laser intensity is defined by the ratio of laser power to the area of the focus spot size. Therefore, the curve has to be refit and the constant k changes to 1.3 MW/cm^2 while constants a and b keep untouched. Although the tested power intensity ranges from 0.5 MW/cm^2 to 9 MW/cm^2, Eqn.9 believed to be applicable at the power intensities higher than 9MW/cm^2.

3.1.3). Intermediate model I
Substituting Eqn.7 or Eqn.8 into Eqn.9, yields a model for the influence of power intensity on absorptivity as follows.

For CW laser, the equation is determined to be:

$$A_{1\text{-}CW} = a - b\exp\left(-\frac{PD^2}{2.98k\pi f^2\lambda^2}\exp\left(-\frac{D^2}{2.98f^2\lambda^2}\left(x^2+y^2\right)\right)\right)$$
(10)

For PW (saw-toothed wave) laser, the governing equation becomes:

$$A_{1\text{-}PW} = \begin{cases} a - b\exp\left(-\frac{PD^2}{1.49k\pi f^2\lambda^2}\frac{\tau(t-m\tau)}{\tau_1(\tau_1+\tau_2)}\exp\left(-\frac{D^2}{1.49f^2\lambda^2}\left(x^2+y^2\right)\right)\right), m\tau < t \le m\tau+\tau_1 \\ a - b\exp\left(-\frac{PD^2}{1.49k\pi f^2\lambda^2}\frac{\tau(m\tau+\tau_1+\tau_2-t)}{\tau_2(\tau_1+\tau_2)}\exp\left(-\frac{D^2}{1.49f^2\lambda^2}\left(x^2+y^2\right)\right)\right), m\tau < t \le m\tau+\tau_1+\tau_2 \\ N/A, m\tau+\tau_1+\tau_2 < t \le (m+1)\tau \end{cases}$$
(11)

This is the intermediate model I, which considers all of the effects of parameters on the left side of the dash line in Fig.1.

3.2). Intermediate model II – effects of material, λ, φ, polarization and T

The effects of material, wavelength, angle of incidence and polarization on absorptivity can be expressed using Eqn.2. Influence of the preheated temperature can be integrated into the model using two methods, which were shown on the right side of the dashed line in Fig.1(a) and Fig.1(b) respectively.

3.2.1). Empirical model
Both empirical models for metals under oxidization free environment and oxidized atmosphere were available.

It was reported that the absorptivity for both steel and aluminum increases linearly as temperature goes up from 20°C to 700°C under the protection of argon gas [8]. Duley et al. [4] presented that for many metals at infrared wavelength in vacuum, the absorptivity at temperature A(T), could be approximated well by the linear relation:

$A_T = A(20°C)[1+B(T-20°C)]$
(12)

Where, B is a constant. Typically, A_T at 1000°C is less than 5 times of A(20°C), and the value of B varies as different metals.

The variation of absorptivity vs. time under oxidized atmosphere at indicated temperatures has also been studied [4, 9]. A theoretical equation was suggested to represent the transient process, which is as follows:

$$A_T(t)=A_T(0)+C(T)R(T)t^{0.5}$$ (13)

Where, $A_T(0)$ represents the absorptivity at temperature T in vacuum; $A_T(t)$ represents absorptivity after oxidation time t at temperature T; C(T) is a constant containing the parabolic rate constant, oxidization film density and the film absorption coefficient; R(T) means reflectivity in vacuum at temperature T.

As seen in Fig.1(a), $A_{P-nk\varphi}$ and $A_{S-nk\varphi}$ can be expressed using Equation 2. After combining the effects of temperature (usually together with oxidization time), the absorptivity can be described as:

$$\begin{cases} A_{P-nk\varphi-T} = A_{P-nk\varphi} \cdot A_T(t) \\ A_{S-nk\varphi-T} = A_{S-nk\varphi} \cdot A_T(t) \end{cases}$$ (14)

If the laser processing is performed in vacuum or at the first shot of laser radiation in air, t is set to zero in Eqn.14. Substituting the actual time passed for laser irradiation at indicated temperature, Eqn.14 can be used as a transient sub-model.

3.2.2). Theoretical model
An alternative way is to treat n/k as function of material, wavelength and temperature so that the absorptivity can be calculated using Eqn.2 directly. Due to the difficulty of obtaining data for n and k at high temperature, a method of relating them to other material properties, such as dielectric constant, $\tilde{\varepsilon}$ was discussed in Ref [4]. Relation between $\tilde{n}$ and $\tilde{\varepsilon}$ can be expressed as:

$$\begin{cases} n = \sqrt{\dfrac{\sqrt{\varepsilon_1^2 + \varepsilon_2^2} + \varepsilon_1}{2}} \\ k = \sqrt{\dfrac{\sqrt{\varepsilon_1^2 + \varepsilon_2^2} - \varepsilon_1}{2}} \end{cases}$$ (15)

It was reported that by using high temperature dielectric measurement techniques, both real portion and imaginary portion of the dielectric constant have been measured as a function of temperature for several mineral ores [12]. The measurements for other materials by using the same technology should be possible.

Substituting Eqn.15 into Eqn.2, yields:

$$
\begin{cases}
A_{P\text{-}nk\varphi T} = \dfrac{4\sqrt{\dfrac{\sqrt{\varepsilon_1^{\,2}+\varepsilon_2^{\,2}}+\varepsilon_1}{2}}}{\left(\left(\sqrt{\dfrac{\sqrt{\varepsilon_1^{\,2}+\varepsilon_2^{\,2}}+\varepsilon_1}{2}}+\dfrac{1}{\cos\varphi}\right)^2+\dfrac{\sqrt{\varepsilon_1^{\,2}+\varepsilon_2^{\,2}}-\varepsilon_1}{2}\right)\cos\varphi} \\[4em]
A_{S\text{-}nk\varphi T} = \dfrac{4\sqrt{\dfrac{\sqrt{\varepsilon_1^{\,2}+\varepsilon_2^{\,2}}+\varepsilon_1}{2}}\cos\varphi}{\left(\sqrt{\dfrac{\sqrt{\varepsilon_1^{\,2}+\varepsilon_2^{\,2}}+\varepsilon_1}{2}}+\cos\varphi\right)^2+\dfrac{\sqrt{\varepsilon_1^{\,2}+\varepsilon_2^{\,2}}-\varepsilon_1}{2}}
\end{cases}
\tag{16}
$$

In this equation, ε_1 and ε_2 are functions of material, wavelength and temperature.

3.3). Generic model

Because no coupling effect exists between two intermediate models obtained above, it is very natural to combine them together by algebraic product operation. The generic model is, therefore, represented as follows.

For CW laser radiation, combining Eqn.10 and Eqn.14, yields:
$$
\begin{cases}
A_{P1} = A_{P\text{-}nk\varphi\text{-}T} \cdot A_{I\text{-}CW} \\
A_{S1} = A_{S\text{-}nk\varphi\text{-}T} \cdot A_{I\text{-}CW}
\end{cases}
\tag{17-1}
$$

Combining Eqn.10 and Eqn.16, yields:
$$
\begin{cases}
A_{P2} = A_{P\text{-}nk\varphi T} \cdot A_{I\text{-}CW} \\
A_{S2} = A_{S\text{-}nk\varphi T} \cdot A_{I\text{-}CW}
\end{cases}
\tag{17-2}
$$

For PW laser radiation, combining Eqn.11 and Eqn.14, yields:
$$
\begin{cases}
A_{P3} = A_{P\text{-}nk\varphi\text{-}T} \cdot A_{I\text{-}PW} \\
A_{S3} = A_{S\text{-}nk\varphi\text{-}T} \cdot A_{I\text{-}PW}
\end{cases}
\tag{17-3}
$$

Combining Eqn.11 and Eqn.16, yields:
$$
\begin{cases}
A_{P4} = A_{P\text{-}nk\varphi T} \cdot A_{I\text{-}PW} \\
A_{S4} = A_{S\text{-}nk\varphi T} \cdot A_{I\text{-}PW}
\end{cases}
\tag{17-4}
$$

3.4). Discussion

As seen in Eqn.17, the generic model consists of two major portions. If power intensity related parameters, such as P, I, TEM and d_{min} are the major concerns, A_{I-CW} or A_{I-PW} can be applied individually. If other parameters, such as n, k, λ, P-/S-, φ and T are the major concerns, $A_{P-nk\varphi T}$ / $A_{P-nk\varphi-T}$ or $A_{S-nk\varphi T}$ / $A_{S-nk\varphi-T}$ can be used individually. At most conditions, some or all of the parameters from each of these two groups are entangled. The generic model, therefore, should be used as a whole equation.

The generic model developed in this paper is good for most forms of laser power intensity distribution. It is capable of including the variation of focal plane relative to the material's surface. For PW laser, the pulse wave can take forms of any function.

Validation of the model needs to be further carried out by experimental means.

4. Simulation of the generic model

In this section, the generic model obtained above was used to simulate the influence of a few factors for both CW and PW lasers.

4.1). Simulation for CW laser radiation

A CW CO_2 laser light was used in this simulation. Other parameters were listed in Table 1.

Table 1 Parameters of simulation for CW laser radiation

Material	N	K	f(mm)	D(mm)	λ(mm)*10^{-3}	P(W)
Carbon steel	5.97	32.2	25.4	3	10.6	500-100,000

4.1.1). Spatial distribution of absorptivity

Distribution of absorptivity for carbon steel at laser power of 1kW, temperature of 20°C and normal incidence was shown in Fig.3.
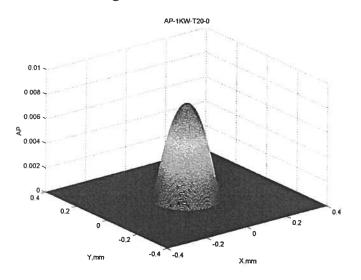

Fig.3 Distribution of absorptivity (P=1kW, T=20°C, φ=0°)

A Gaussian beam has a power intensity that is highest at the center and drops off exponentially as the spatial dimensions increases. The absorptivity is higher at high power intensity and drops exponentially as the intensity decreases. This is the reason why the distribution of the absorptivity resembles a somewhat steeper Gaussian distribution in this simulation.

When power level increases to 5 kW, the absorptivity continues to resemble the steep Gaussian distribution. However, the central area is flattened due to saturation that is seen in Fig.4. In addition, the distribution expands radially at increased power levels.
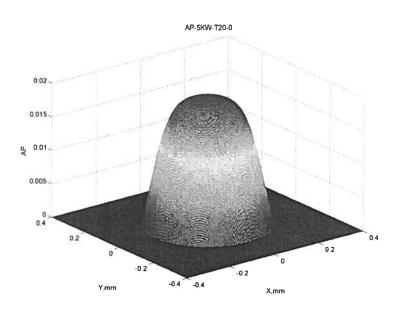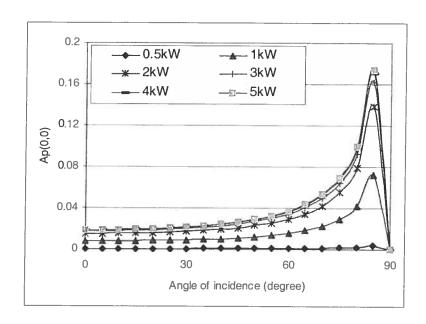
Fig.4 Distribution of absorptivity (P=5kW, T=20°C, φ=0°)

4.1.2). Absorptivity at the spot center

The variation of absorptivity at the center of the spot, A(0,0) for both P-ray and S-ray versus angle of incidence, φ is shown in Fig.5 for several power levels. When φ is equal to zero, A(0,0) is the same for P-ray and S-ray. As φ increases, A(0,0) for S-ray decreases smoothly until it becomes zero at 90°. A(0,0) for P-ray increases to the maximum value at Brewster angle. Beyond this angle, it decreases sharply until it becomes zero at 90°. This phenomenon agrees well with the literatures [1, 7].

As shown in Fig.5, the absorptivity is low at low power levels and increases rapidly as power increases until 3kW. No obvious increase was observed beyond this power level. Therefore, increasing laser power beyond 3kW (keeping other parameters constant) is not beneficial for increasing the absorptivity in this simulation.
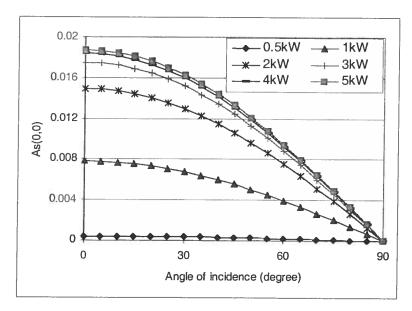
Fig.5 Absorptivity vs. angle of incidence under different power levels

4.1.3). Diameter of the absorptivity distributed zone

Diameter of the absorptivity distributed zone, D_{adz} is defined by the diameter of the zone with energy absorption under normal incidence of laser. Theoretically, it is equal to the diameter of the zone within which the absorptivity is above zero. In calculation with a computer, the smallest positive number the computer may reach, eps, was chosen to replace 0 in order to avoid overflow.

The relative diameter, D_{adz}/d_{min} is an important parameter which reveals the area of the absorption distributed zone compare to the focal spot size. Value of d_{min} can be obtained using Eqn.5, which is equal to 0.219mm for CW laser. As shown in Fig.6, D_{adz}/d_{min} increases with

increased power sharply in the range from 0.5kW to 3kW. Beyond 3kW, the rate of increase slows down significantly.
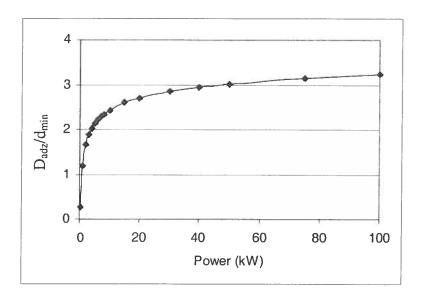

Fig.6 Effect of power on D_{adz}/d_{min}

4.1.4). Critical value of the power

In order to make energy coupling between laser and material surface possible, the laser power should not be less than a threshold. Let $A_{1-cw} \geq 0$ in Eqn.10, we can obtain the critical value by solving the problem as follows.

$$\begin{cases} \min(P) \\ A_{1-cw} \geq 0 \end{cases} \tag{21}$$

For the parameters used in this simulation, the minimum value of P is found to be 478 Watts.

4.2). Simulation for PW laser radiation

A Nd:YAG laser that outputs a pulse wave as shown in Fig.2, was used in this simulation. Other parameters used were listed in Table 2.

Table 2 Parameters of simulation for PW laser radiation

Material	N	K	f(mm)	D(mm)	λ(mm) $*10^{-3}$	$\overline{P}$(W)	τ_1(s) $*10^{-6}$	τ_2(s) $*10^{-6}$	τ (s) $*10^{-3}$
Carbon steel	3.81	4.49	25.4	3	1.06	0.01	20	80	10-300

4.2.1). Spatial distribution of absorptivity

As shown in Fig.7 and Fig.8, the distribution of the absorptivity resembles a steep Gaussian distribution, which is similar to Fig.3 and Fig.4. The absorptivity is low at low power intensity and becomes saturated at high level.
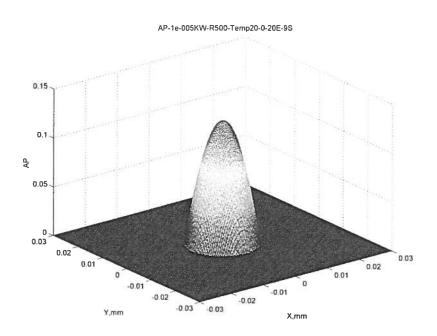

Fig.7 Distribution of absorptivity (T=20°C, $\varphi=0°$, τ =50ms, t=20μs).
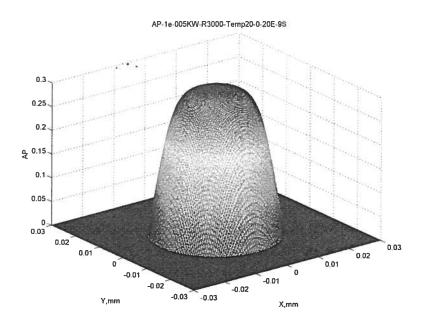

Fig.8 Distribution of absorptivity (T=20°C, $\varphi=0°$, τ =300ms, t=20μs)

Because focal spot size, d_{min} is equal to 0.0219mm in this condition, the absorptivity-distributed zone is equivalent to 1% of that for CW laser. The laser energy distributed in a very small area and therefore, the power intensity is very high. This is one reason why a low average power, 0.01W in this simulation can result in a power intensity high enough to make energy coupling possible. The other reason is that the laser energy was supplied in a relative short time, which is about 1/500 or 1/3000 of the whole pulse period, causing a very high power intensity during the radiation period.

4.2.2). Variation of A(0,0) with time
The variation of absorptivity at central point with time under different pulse cycle was demonstrated in Fig.9. When period, τ increases in the range from 25ms to 300ms, the absorptivity increases with time from 0 to 20μs and decreases from 20μs to 100μs, corresponding very well to the variation of the saw-toothed laser power input. Noted that the shorter the radiation time is, the higher is the power intensity. When τ increases to 300ms, the pulse energy was supplied in a very short time, 1/3000 of the period. At this power intensity, the absorptivity becomes saturated (about 0.3). Also, time used for A to increases from 0 to saturation and decreases from saturation to 0 was significantly reduced. It could be treated as a window function (i.e., treat A as a constant when time changes from 0 to $\tau_1 + \tau_2$) in order to facilitate the successive modeling of thermal transfer for laser processing procedure.
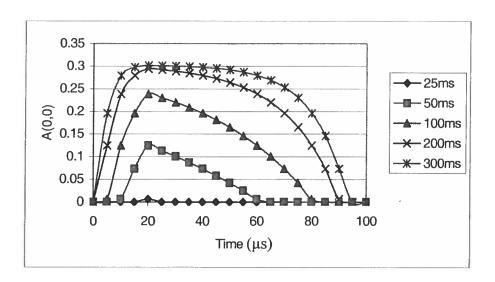

Fig.9 A(0,0) vs. time under different pulse cycle

Noted that the volume of absorptivity is determined by the volume of $\frac{\tau_1}{\tau}$ and $\frac{\tau_2}{\tau}$, regardless of the actual period of time and thus, is irrelevant to the energy supplied within each pulse.

4.2.3). Variation of D_{adz}/d_{min} with time

The variation of D_{adz}/d_{min} with time under different pulse cycle was shown in Fig.10. D_{adz}/d_{min} is a power dependent parameter, which varies with time as the same way as power. It increases in the range from 0 to 20μs and decreases from 20μs to 100μs.
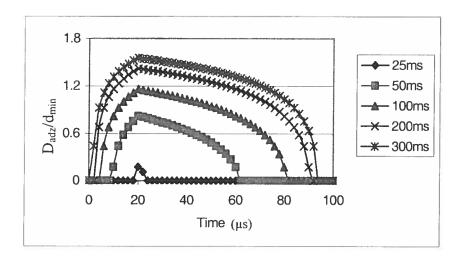

Fig.10 D_{adz}/d_{min} vs. time under different pulse period

4.3). Discussion

In these case studies, the spatial distribution of absorptivity for both PW and CW laser is a steep Gaussian distribution. The top center flats out when power reaches 3kW for CW laser and when pulse period reaches 300ms for PW laser light. The power intensity in these conditions is 8×10^4 W/mm^2 for CW and 15.9×10^4 W/mm^2 for PW respectively. This is the desirable volume of power intensity, $8 - 15.9 \times 10^4$ W/mm^2, for obtaining the maximum value of absorptivity. Increasing the power density beyond this value will not increase the absorptivity further.

The variation of D_{adz}/d_{min} with power intensity for PW laser light and CW laser light was shown in Fig.11. The power intensity was defined by the quotient of laser power divided by the area of focal spot size. The power at the time point of 20μs is used for PW laser light. It is seen that the power density is an essential parameter, which determines the magnitude of D_{adz}/d_{min}, rather than the power itself. It is also seen from these case studies that under the same power intensity, the magnitude of D_{adz}/d_{min} for PW is lower than that for CW. This reveals that the laser energy is more concentrated for a laser with shorter wavelength.
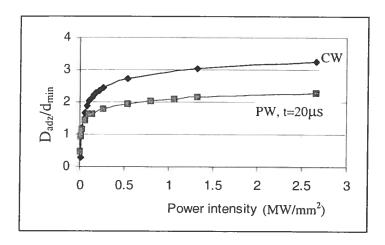
Fig.11 D_{adz}/d_{min} vs. power intensity for CW laser and PW laser

5. Conclusions

A generic model which concerns the comprehensive effects of numerous parameters has been developed in this paper. This generic model consists of two intermediate models. One of them affects the magnitude of absorptivity, while the other has an influence on the area of the absorptivity distributed zone. Usually, the generic model is used as a whole. Sometimes, either of the intermediate models can be applied independently when indicated parameters are not entangled.

The model is developed using a generic methodology and thus is expected to be applicable in general conditions. Simulation results using the generic model agree well with the literatures. Further validation is necessary and will be made by experiments.

Case studies for simulation of generic model have been executed, some findings were found:
1). Power intensity is an important parameter, which has a substantial influence on both the magnitude of absorptivity and the area of absorptivity distributed zone.
2). Absorptivity is power intensity dependent, but is regardless of the amount of energy supplied to the material surface.
3). There is an economic power level for obtaining the maximum energy coupling efficiency.
4). Energy coupling efficiency is usually higher at shorter laser wavelength, keeping other conditions constant.

References

1. Steen WM. Laser material processing (2nd edition). Springer-Verlag London Limited, UK, 1998.
2. Ricciardi G and Cantello M. Laser material interaction: absorption coefficient in welding and surface treatment. Annals of the CIRP. 1994; 43(1): 171-175.
3. Duley WW. Laser welding. A Wiley-Interscience Publication, USA, 1999.
4. Duley WW. Laser material interactions of relevance to metal surface treatment. In Draper CW and Mazzoldi P (eds): Laser material treatment of metals. Martinus Nijhoff Publishers, Dordrecht, 1986.
5. Columbia University. Combined Research and Curriculum Development Nontraditional Manufacturing (NTM) – Laser Machining Processes (LMP) on-line curriculum @ http://www.columbia.edu/cu/mechanical/mrl/ntm/level2/ch05/html/l2c05s04.html
6. Edward JS and Sun Y. New laser processing techniques for thick- & thin-film circuit manufacturing. Electro Scientific Industries, Inc. Portland. PDF file @ http://www.esi.com/careers/pdfs/sun_swenson.pdf
7. Migliore L. Laser materials processing. Marcel Dekker Inc. New York, 1996.
8. Dekumbis R., Mayer H. and Fernandez P. A fast experimental method of measuring laser beam absorption as a function of temperature in solids. 3rd international conference on lasers (iitt). Kongresshaus, Zurich, 1987. 289-296.
9. Duley W., Semple D., Morency J., et al. Coupling coefficient for cw CO_2 laser radiation on stainless steel. Optics laser technology. 1979; 11:313-316.
10. Fuerschbach PW. Measurement and prediction of energy transfer efficiency in laser beam welding. Welding Journal-Welding Research Supplement. 1996; 75(1): 24-34.
11. Juptner W, Franz Th, Sikau J, et al. Laser interaction with plasma during material processing. Laser physics. 1997; 7(1): 202-207.
12. Atomic Energy of Canada Limited. Microwaves and minerals. Ministry of Northern Development and Mines, Mines and Minerals Division, Mineral Development and Lands Branch, Toronto, CA, 1990.